Supplementary methods

Detection of ROS by fluorescent indicators. We treated PC12 cells with 10 μM of 5-(and-6)-chloromethyl-2',7'-dichlorodihydroflurescein diacetate, acetyl ester (CM-H_2DCFDA) (purchased from Molecular Probes), 5 μM diaminofluorescein-2 diacetate (DAF-2 DA) (purchased from Daiichi Pure Chemicals Co.), or 5 μM of 2-[6-(4'-hydroxy)phenoxy-3*H*-xanthen-3-on-9-yl]benzoate (HPF) (Daiichi Pure Chemicals Co.) for 30 min to detect cellular H_2O_2, NO• or •OH, respectively. We took fluorescent images with a laser-scanning confocal microscope (Olympus FV300) using excitation and emission filters of 488 nm and 510 nm, respectively. HPF can be specifically oxidized by •OH, peroxynitrite ($ONOO^-$) and lipid peroxides, but neither H_2O_2, NO• nor O_2^-•[14]. For the detection of cellular O_2^-•, we used 0.5 μM MitoSOX (purchased from Molecular Probes), and took images using excitation and emission filters of 543 nm and 565 nm, respectively.

Staining of mitochondria. For staining of mitochondria, we co-stained with MitoTracker Green (MTGreen) (1 μM; Molecular Probes) and tetramethylrhodamine methyl ester (TMRM) (100 nM; Molecular Probes). Fluorescence from MTGreen is independent of the membrane potential, whereas that from TMRM is sensitive to the membrane potential. MTGreen and TMRM were detected using excitation at 488 and 543 nm, and emission filters of 510 and 565 nm, respectively.

Immunostaining. We purchased antibodies against HNE and 8-OH-G from Nikken Seil Co, and antibodies against TUJ-1[24] and GFAP from COVANCE and ThermoImmunon, respectively. We used BODIPY FL goat anti-mouse IgG (Molecular Probe) as a secondary antibody and visualized signals with a laser-scanning confocal microscope.

The intracellular Fenton reaction. We preincubated PC12 cells with 1 mM $CuSO_4$ for 30 min in medium containing 1% FCS, washed once with phosphate-buffered saline containing $CaCl_2$ (0.1 g/l), $MgCl_2.6H_2O$ (0.1 g/l), glucose (1g/l) and sodium pyruvate (0.036 g/l) (pH 7.2), and then exposed to the indicated concentration of ascorbate (vitamin C) for 1 h in the phosphate-buffered saline that was described above. As negative controls, $CuSO_4$ or ascorbate was omitted. Note that Cu^{+2} is reduced by ascorbate to Cu^+, which catalyzes the Fenton reaction to produce •OH from H_2O_2 that is being spontaneously produced in the cells.

Electron spin resonance measurement. We used *5,5*-dimethyl-1-pyrroline *N*-oxide (DMPO) as a free radical trapper, and detected electron spin resonance (ESR) signals with a KEYCOM ESR spectrometer type ESR-X01. As a standard of the reactant of •OH with DMPO, we produced •OH by the Fenton reaction in the mixture of 0.1 mM H_2O_2 and 1 mM $FeCl_2$ in the presence of 0.1 mM DMPO and subjected the whole solution ESR measurement. For the measurements, we normalized sensitivity of each experiment with the strength of internal ESR signal derived from Mn^{2+}. To obtain a spectrum, ESR was scanned for 2 min, accumulated 10 times, and all signals were averaged.

For H_2 treatment, we prepared media containing 0.6 mM H_2 and 8.5 mg/l O_2, and filled a closed culture flask with 80% H_2 and 20% O_2 gas. We pretreated PC12 cells (2×10^6 cells / 25 cm^2 flask) with 0.1 M DMPO and 2 mM $CuSO_4$ in DMEM containing 1% FCS for 30 min at 37 °C in the presence or absence of 0.6 mM H_2. After the removal of this medium, we exposed the cells to 0.2 mM ascorbate and 0.1 mM H_2O_2 in 0.3 ml of PBS for 5 min at room temperature to produce •OH by the Fenton reaction, and scraped the cells into a flat cuvette for ESR measurement. In the other method, we preincubated PC12 cells (2×10^6 cells / 25 cm^2 flask) in 0.3 ml of PBS containing 0.1 M DMPO and 30 μg/ml antimycin A for 7 min at room temperature in the absence or presence of 0.6 mM H_2, then scraped the cells into a flat cuvette for ESR measurement. A differential spectrum was obtained by digitally subtracting one spectrum from the other to visualize the signals decreased by H_2 treatment.

Primary culture. We prepared primary cultures of neocortical neurons from 16-day rat embryos by the method described previously[28]. In brief, neocortical tissues were cleaned of meninges, minced, and treated with protease cocktail (SUMILON). After mechanical dissociation by pipetting, we resuspended cells in nerve-cell culture medium (SUMILON), and then plated onto poly-L-lysine-coated plates at a density of 5×10^4 cells / cm^2, changed the Neurobasal Medium (Invitrogen) with B-27 (Invitrogen) once every three days and then used neurons at day 11. One d before OGD, we changed the medium to Neurobasal Medium with B-27 minus AO (Invitrogen), and confirmed neuronal identity by immunostaining with antibodies to neuron marker TUJ-1, and astrocyte marker GFAP. We used preparations if only containing over 90% neurons for experiments.

Oxygen-glucose deprivation. To initiate OGD, we replaced the culture medium with a glucose-deficient DMEM from which O_2 had been removed by bubbling in a mix of either 95% N_2 / 5% CO_2 or 95% H_2 / 5% CO_2 and maintained the culture for 60 min at 30 °C under an

atmosphere of either 95% nitrogen / 5% CO_2 or 95% H_2 / 5% CO_2. Treatment was terminated by exchanging the experimental medium with stocked culture medium and further incubation at 37 °C with 95% air / 5% CO_2.

Reaction of H_2 in cell-free systems. We performed fluorescence spectroscopic studies with a Shimadzu RF-5300PC. For solution studies, we dissolved H_2 in water beyond the saturated level under 0.4 MPa of hydrogen pressure for 2 h and then used under atmospheric pressure. We determined H_2 concentrations with a hydrogen electrode in each experiment.

To detect the reaction of H_2 with the oxidized form of cytochrome *c*, FAD, or NAD^+, we incubated solutions containing 10 μM cytochrome *c*, 1 mM FAD or 1mM NAD^+ with or without 0.8 mM H_2 in a closed cuvette at 23 °C for 30 min, and observed no reaction by absorbance at 415, 400 and 340 nm, respectively.

We monitored the reactivity of H_2 with various ROS by HPF, DAF-2, or nitroblue tetrazolium (NBT). We measured fluorescent signals of HPF and DAF-2 at 515 nm with excitation at 490 and 495 nm, respectively, while the reduction of NBT to NBT-diformazan by absorbance at 550 nm.

To detect the reaction of H_2 with •OH, we mixed hydrogen solution, phosphate buffer (10 mM at pH 7.4), ferrous perchlorate (0.1 mM), and HPF (0.4 μM). We initiated the Fenton reaction by adding H_2O_2 to 5 μM in a closed cuvette at 23 °C with gentle stirring and monitored fluorescence for 30 s.

To detect the reaction of H_2 with O_2^-•, we mixed solutions containing xanthine and NBT (supplied by TREVIGEN) with or without 0.8 mM H_2 in a closed cuvette, and initiated the reaction by adding xanthine oxidase at 23 °C and monitored for 5 min.

To detect the reaction of H_2 with H_2O_2, we incubated solutions including phosphate buffer (10 mM at pH 7.4) and H_2O_2 (10 μM) with or without H_2 (0.8 mM) in a closed glass tube at 23 °C for 30 min. We converted remaining H_2O_2 to •OH by 0.2 μM horseradish peroxidase and then incubated with 10 μM HPF for 5 min.

To detect the reaction of H_2 with NO•, we incubated solutions containing phosphate buffer (10 mM at pH 7.4) and 1-hydroxy-2-oxo-3-(*N*-methyl-3-aminopropyl)-3-methyl-1-triazene (NOC7, 0.1 μM, purchased from Dojin Chemicals Co.) with or without 0.8 mM H_2 in a closed cuvette at 23 °C for 30 min, and monitored the remaining NO• by incubation with 5 μM DAF-2 for 10 min.

To detect the reaction of H_2 with peroxynitrite ($ONOO^-$), we diluted a stock solution of 1 μM $ONOO^-$ in alkali 200-fold into 10 mM phosphate buffer with 0.4 μM HPF in the presence or absence of 0.8 mM H_2, and then examined HPF signals after 23 °C for 1 min.

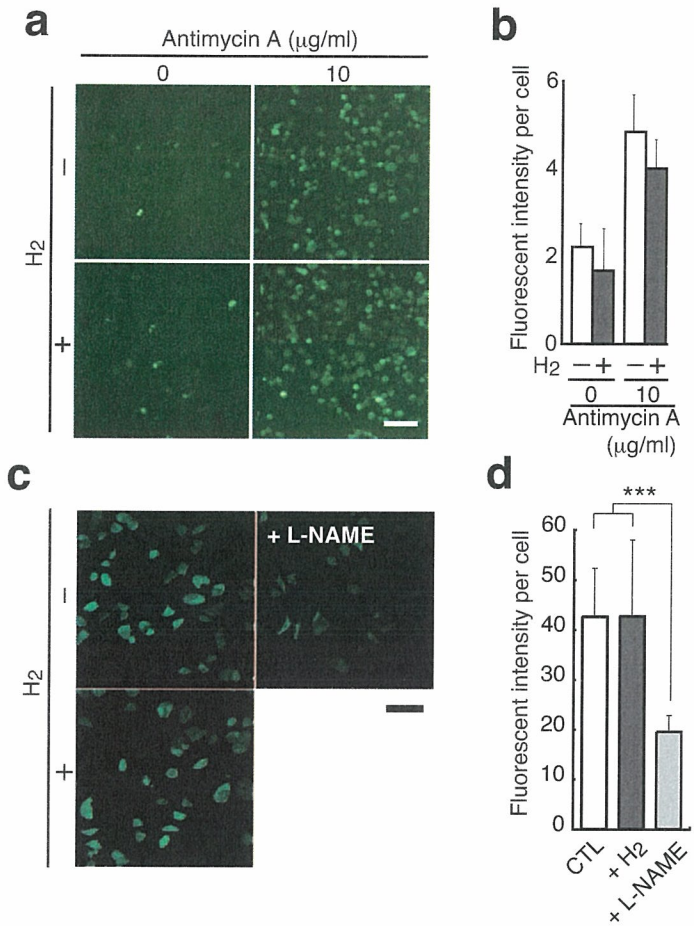

Supplementary Figure 1 Molecular hydrogen dissolved in culture medium does not reduce cellular hydrogen peroxide and nitric oxide.

(**a**) PC12 cells were held in medium with or without 0.6 mM H_2, and antimycin A (10 μg/ml) was added to the medium to induce O_2^{-}•, which would be rapidly converted into H_2O_2. Representative laser-scanning confocal images of the fluorescence of H_2O_2 marker 2',7'-dichlorodihydroflurescein (H_2DCF) were taken 1 h after the addition of antimycin A. Scale bar: 100 μm. (**b**) DCF fluorescence in cells treated with antimycin A in the presence or absence of 0.6 mM H_2 was quantified from 100 cells from each independent experiment using NIH Image software (mean ± SD, n = 4). (**c, d**) Cellular NO• was detected with a cellular NO•-specific fluorescent probe, DAF-2 DA (diaminofluorescein-2 diacetate, purchased from Daiichi Pure Chemicals Co.) by laser-scanning confocal microscopy using excitation and emission filters of 488 and 510 nm, respectively. As a negative control, an inhibitor of NOS (L-NAME: N^G-Nitro-L-arginine methyl ester, purchased from Sigma) was added not to generate NO•. Scale bar: 50 μm. (**d**) DAF-2 DA fluorescence was quantified as described in (**b**) (mean ± SD, n = 5). ***$P < 0.001$.

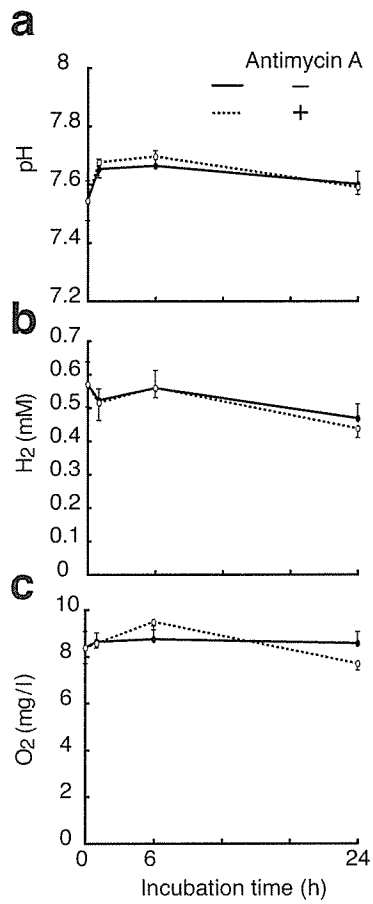

Supplementary Figue 2 pH, H_2 and O_2 maintain constant in culture medium in a closed flask filled with a mixed gas.

DMEM culture medium with dissolved H_2 and O_2 was prepared as described in **Methods**. PC12 cells (5×10^5) were cultured in the medium with or without antimycin A (10 μg/ml) in a closed culture flask (25 cm^2) filled with a mixed gas composed of 75% of H_2, 20% of O_2 and 5% of CO_2. At the indicated time, pH, H_2 or O_2 in the medium was monitored with a pH meter, H_2 or O_2 electrode. One flask was used for one measurement. Data show the mean ± SD (n = 4).

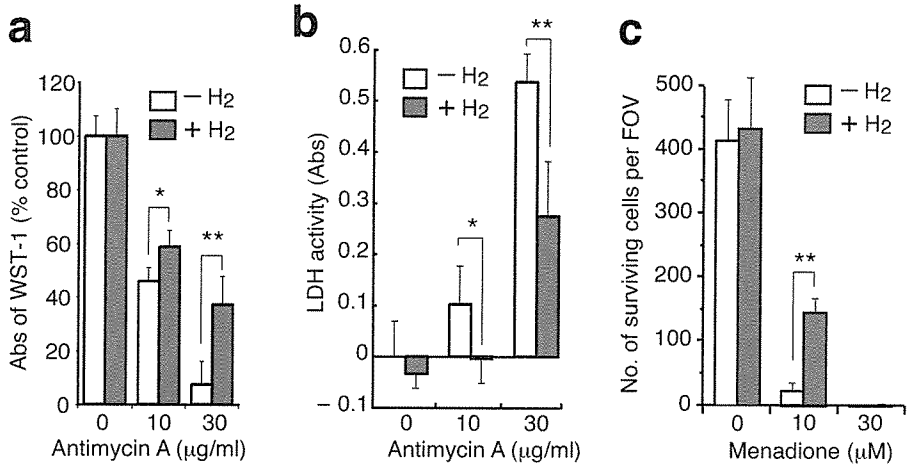

Supplementary Figure 3 Several methods confirm protection of cells by H_2 against oxidative stress.

PC12 cells incubated in the presence of or absence of 0.6 mM H_2 were treated with the indicated concentration of antimycin A (**a**, **b**) or menadione (**c**), and maintained with each H_2 concentration for 24 h as described in **Methods**. (**a**) As another method, a modified MTT assay (WST-1 assay) were applied to the cell system according to a Cell Counting Kit (purchased from Wako) to ensure the protective effect by H_2 against oxidative stress (mean ± SD, $n = 4$). $^*P < 0.05$, $^{**}P < 0.01$. (**b**) Lactate dehydrogenase (LDH) activities were measured to estimate cellular LDH leakage from damaged cells according to LDH-Cytotoxic Test kit (Wako). LDH activity in medium of antimycin A- and H_2-untreated cells was taken as the background (mean ± SD, $n = 4$). $^*P < 0.05$, $^{**}P < 0.01$. (**c**) Instead of antimycin A, menadione was used to induce oxidative stress for 24 h and living cells were enumerated as described in **Fig. 2f** (mean ± SD, $n = 4$). $^{**}P < 0.01$.

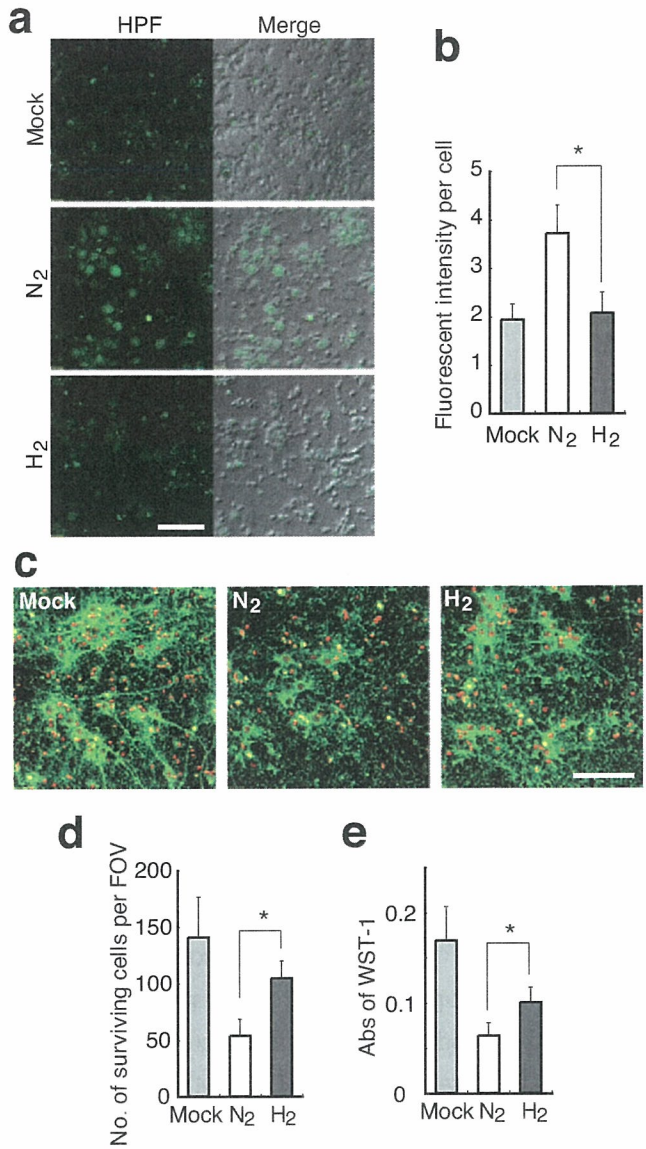

Supplementary Figure 4 Molecular hydrogen protects cultured neurons from ischemia and reperfusion *in vitro*.

A primary culture of rat neocortical cells was prepared and subjected to OGD (oxygen glucose deprivation) as described in **Supplementary methods**. (**a**) Ten min after reperfusion, cells were stained with HPF (left, fluorescent images; right, superimposition of the fluorescent HPF images with Nomarski differential interference contrast images). "Mock" indicates that cells were treated with DMEM medium containing glucose and oxygen instead of being subjected to OGD. Scale bar: 100 μm. (**b**) The average fluorescent intensity of HPF was measured in 100 cells (mean ± SD, $n = 4$). *$P < 0.05$. (**c**) Twenty hours after OGD, surviving neurons were fixed and immunostained with the neuron-specific antibody to TUJ-1 (green) and with PI (red). Scale bar: 100 μm. (**d**) Dead cells were washed out in the staining procedure and living cells were enumerated under a fluorescent microscope in four fields of view (FOV) per well (mean ± SD, $n = 4$). *$P < 0.05$. (**e**) Twenty hours after OGD, viability in a well was estimated by a modified MTT viability assay according to a Cell Counting Kit (WST-1 assay) (mean ± SD, $n = 4$). *$P < 0.05$.

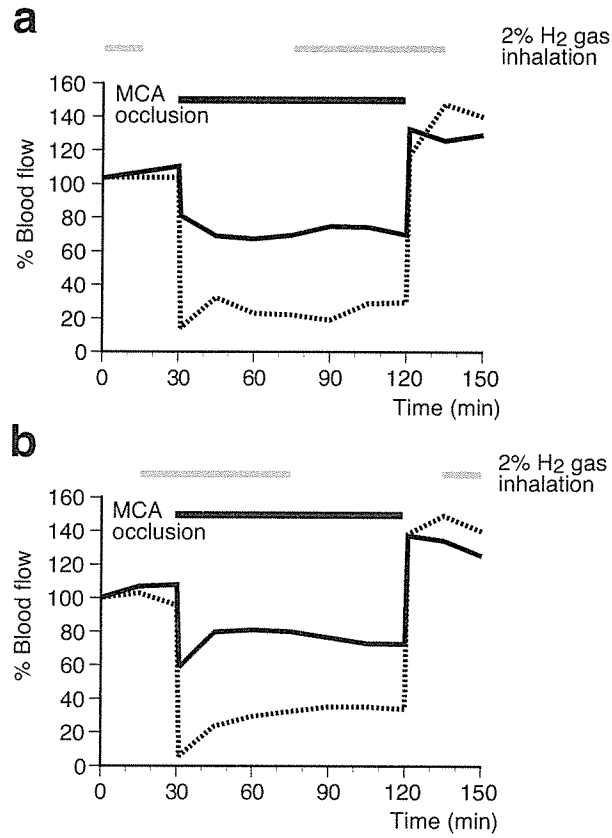

Supplementary Figure 5 Cerebral blood flow is not influenced by H_2 inhalation.

Middle cerebral artery occlusion was produced as described in **Methods.** Cerebral blood flow was measured by laser Doppler flowmetry using an ALF21 (ADVANCE Co.) at 2 mm lateral to the bregma for penumbra (solid line) and 5 mm lateral to the bregma for ischemic core (dotted line). Periods of 2% H_2 inhalation and middle cerebral artery (MCA) occlusion are shown by grey and solid thick lines, respectively.

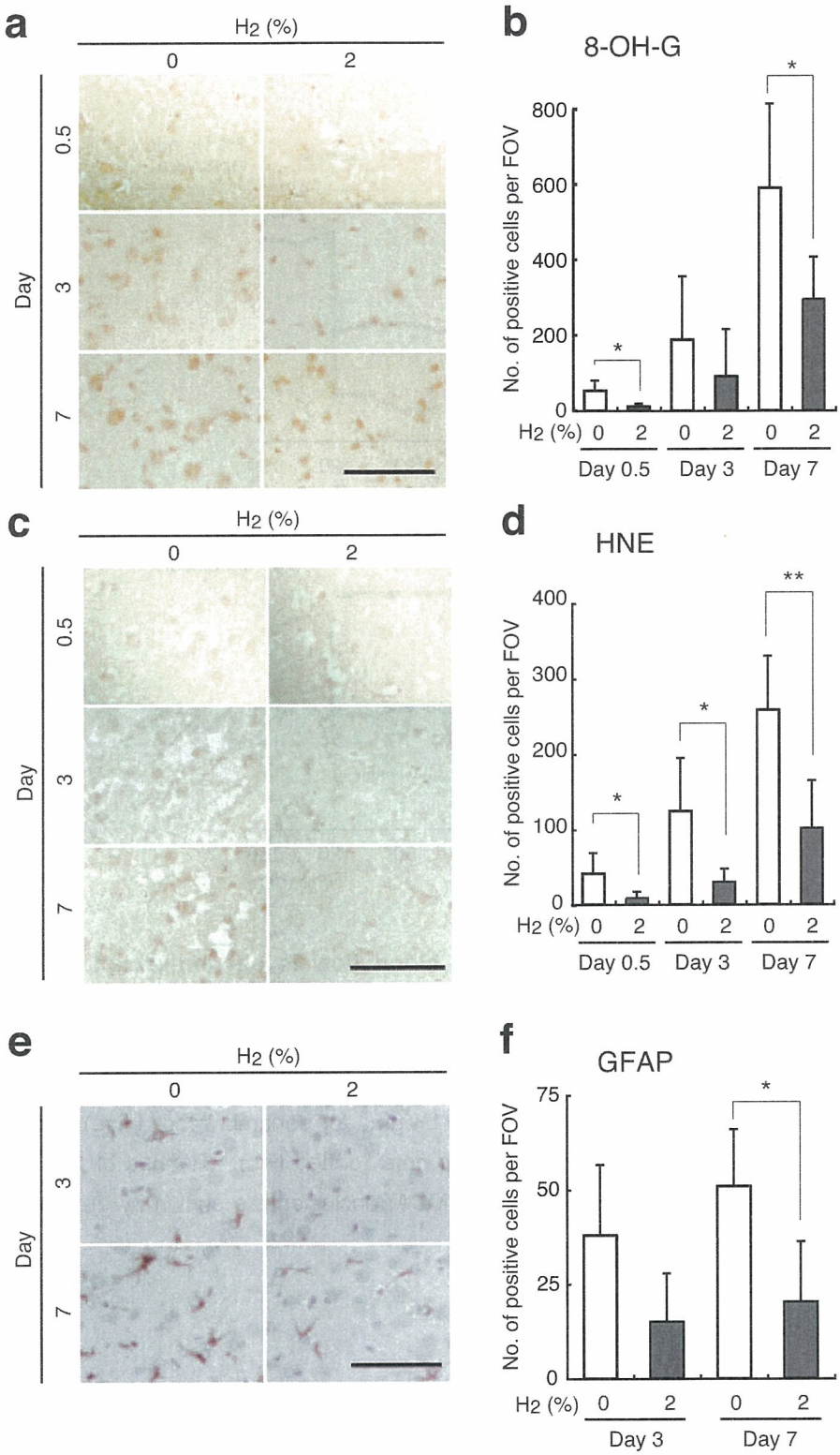

Supplementary Figure 6 The brain after induction of ischemia reperfusion injury with or without H_2 treatment were immunostained.

Twelve h (0.5 d), 3 or 7 d after MCA occlusion, the brains were fixed and embedded in paraffin. Coronal 6-μm-sections were stained with antibody to 8-OH-G in the ischemic penumbra area in the temporal cortex (**a**), with antibody to HNE in the ischemic penumbra area in the temporal cortex (**c**), and with antibody to GFAP at the ischemic penumbra area in the occipital cortex (**e**). Scale bar: 100 μm. Positive cells with antibodies to 8-OH-G (**b**), HNE (**d**) and GFAP (**f**) per field of view (FOV) were counted in exactly the same regions in a blinded manner (mean ± SD, $n = 6$). $^{*}P < 0.05$, $^{**}P < 0.01$.

Supplementary Table Physiological parameters during cerebral ischemia reperfusion

preischemia							ischemia						
0% H_2							**0% H_2**						
No.	temp. (°C)	pH	pCO_2	pO_2	glucose (mg/dl)	pressure (mmHg)	No.	temp. (°C)	pH	pCO_2	pO_2	glucose (mg/dl)	pressure (mmHg)
1	37.4	7.47	39	107	120	110	1	37.4	7.42	44	89	130	145
2	37.5	7.39	51	113	114	95	2	37.1	7.40	51	98	117	120
3	37.5	7.47	43	109	119	108	3	37.4	7.44	47	115	115	130
4	37.4	7.46	43	134	120	110	4	37.0	7.42	48	119	117	150
5	37.1	7.44	40	109	103	110	5	37.5	7.42	42	113	105	150
6	37.2	7.45	39	125	110	120	6	37.5	7.44	41	112	105	153
Average	37.4	7.45	43	116	114	109	Average	37.3	7.42	46	108	115	141
S.D.	0.2	0.03	5	11	7	8	S.D.	0.2	0.02	4	12	9	13
2% H_2							**2% H_2**						
1	37.1	7.45	46	130	109	105	1	37.3	7.41	48	111	120	120
2	37.4	7.44	50	118	104	87	2	37.6	7.43	43	99	97	135
3	37.7	7.40	46	105	114	103	3	37.8	7.42	45	104	100	150
4	36.9	7.45	47	121	107	100	4	37.0	7.39	52	97	105	150
5	37.5	7.46	41	120	109	100	5	37.3	7.41	45	109	107	145
6	37.0	7.46	45	114	107	115	6	37.5	7.42	47	108	113	160
Average	37.3	7.44	46	118	108	102	Average	37.4	7.41	47	105	107	143
S.D.	0.3	0.02	3	8	3	9	S.D.	0.3	0.01	3	6	8	14
4% H_2							**4% H_2**						
1	37.6	7.48	36	118	113	120	1	37.0	7.40	48	110	105	145
2	37.2	7.45	40	134	96	112	2	36.8	7.40	46	107	94	120
3	37.6	7.46	43	119	90	125	3	37.0	7.41	47	83	91	130
4	36.7	7.46	39	128	103	120	4	37.6	7.43	43	111	97	145
5	36.8	7.43	45	111	97	120	5	37.4	7.45	44	105	100	140
6	37.5	7.49	34	127	103	100	6	37.4	7.44	46	110	105	150
Average	37.2	7.46	40	123	100	116	Average	37.2	7.42	46	104	99	138
S.D.	0.4	0.02	4	8	8	9	S.D.	0.3	0.02	0	11	6	11

reperfusion for 15 min							reperfusion for 30 min						
0% H_2							**0% H_2**						
No.	temp. (°C)	pH	pCO2	pO2	glucose (mg/dl)	pressure (mmHg)	No.	temp. (°C)	pH	pCO2	pO2	glucose (mg/dl)	pressure (mmHg)
1	37.3	7.39	45	101	132	155	1	37.5	7.41	41	110	135	140
2	37.2	7.40	52	94	108	135	2	37.4	7.40	49	97	111	130
3	37.3	7.46	44	105	113	135	3	37.0	7.40	51	109	115	118
4	37.5	7.43	46	119	116	153	4	37.5	7.42	46	99	118	135
5	37.2	7.40	44	122	104	155	5	37.1	7.43	40	134	105	130
6	37.7	7.41	43	107	105	140	6	37.7	7.35	50	93	97	110
Average	37.4	7.42	46	108	113	146	Average	37.4	7.40	46	107	114	127
S.D.	0.2	0.03	3	11	10	10	S.D.	0.3	0.03	5	15	13	11
2% H_2							**2% H_2**						
1	37.5	7.42	42	107	120	120	1	37.4	7.39	45	116	115	100
2	37.5	7.41	45	98	100	95	2	37.4	7.43	42	97	103	90
3	37.2	7.40	46	109	111	150	3	37.0	7.38	48	117	112	150
4	37.4	7.39	49	100	110	108	4	37.3	7.36	53	109	110	110
5	37.3	7.40	45	108	107	130	5	37.5	7.37	46	119	107	95
6	37.1	7.39	49	113	105	130	6	37.2	7.38	51	115	109	125
Average	37.3	7.40	46	106	109	122	Average	37.3	7.39	48	112	109	112
S.D.	0.2	0.01	3	6	7	19	S.D.	0.18	0.02	4	8	4	23
4% H_2							**4% H_2**						
1	37.4	7.39	49	103	111	140	1	37.1	7.43	37	142	107	125
2	37.3	7.36	49	93	96	120	2	37.4	7.29	41	133	96	112
3	37.4	7.39	46	90	92	135	3	37.5	7.39	47	93	90	135
4	37.4	7.41	45	113	96	145	4	37.4	7.39	45	134	100	130
5	37.1	7.43	45	107	98	140	5	37.1	7.40	44	138	100	125
6	37.3	7.42	44	120	97	150	6	37.1	7.40	47	143	94	140
Average	37.3	7.40	46	104	98	138	Average	37.3	7.38	44	131	98	128
S.D.	0.12	0.03	2	12	7	10	S.D.	0.19	0.05	4	19	6	10

Journal of Alzheimer's Disease 9 (2006) 155–166
IOS Press

Dysfunction of mitochondria and oxidative stress in the pathogenesis of Alzheimer's disease: On defects in the cytochrome *c* oxidase complex and aldehyde detoxification

Shigeo Ohta* and Ikuroh Ohsawa
Department of Biochemistry and Cell Biology, Institute of Development and Aging Sciences, Graduate School of Medicine, Nippon Medical School, 1-396 Kosugi-cho, Nakahara-ku, Kawasaki-city, Kanagawa-pref., 211-8533 Japan

Abstract. The mitochondrion is an organelle that plays a central role in energy production. It, at the same time, generates reactive oxygen species as by-products. Large-scale epidemiological case-control studies suggest the involvements of dihydrolipoamide succinyltransferase (DLST) of the mitochondrial Krebs cycle and mitochondrial aldehyde dehydrogenase-2 (ALDH2) in Alzheimer's disease (AD). The *DLST* gene has two gene-products, one of which, a novel gene product MIRTD, mediates the molecular assembly of the cytochrome *c* oxidase complex whose defect has been a candidate of the causes of AD. Since levels of MIRTD mRNA in the brains of AD patients were significantly low, a decrease in MIRTD could affect energy production. ALDH2, a matrix enzyme, was found to act as a protector against oxidative stress through oxidizing toxic aldehydes, such as 4-hydroxy-2-nonenal, that are spontaneously produced from lipid peroxides. Hence, a decrease in ALDH2 activity is proposed to contribute to AD. Indeed, transgenic mice with low activity of ALDH2 exhibited an age-dependent neurodegeneration accompanying memory loss. Since amyloid β peptide has been recently shown to be present in neuronal mitochondria to decline energy production and enhance ROS production, it has become possible to link AD more closely with roles of mitochondria in the pathogenesis.

Keywords: Aldehyde, ALDH2, case-control study, cytochrome *c* oxidase, DLST

1. Introduction

The mitochondrion has been recognized as an organelle whose function is specific in energy metabolism. It oxidizes substrates such as carbohydrates, fatty acids, and amino acids through multiple steps and reduces NAD^+ and FADH. Using this reductive energy, it performs oxidation-reduction reactions through a series of the electron transfer system. The electrochemical potential across the mitochondrial inner membrane provides energy for ATP synthesis. At the same time, superoxide radicals are generated from oxygen molecules by accepting electrons that have been released from the electron transfer system. The other reactive oxygen species (ROS), hydrogen peroxide and hydroxyl radical were converted from superoxide radicals. Thus, mitochondria are the largest source of ROS [1].

In addition to the role of energy metabolism, mitochondria have essential roles in apoptosis by storing the initiation signal factor, regulatory factors, and execution factors and releasing these factors during apoptosis. Moreover, mitochondria store calcium and regulate cell death by controlling calcium concentration. A decline in energy production disturbs homeostasis in the cell and induces cell death due to necrosis. In

*Corresponding author. Fax: +81 44 733 9268; E-mail: ohta@nms.ac.jp.

ISSN 1387-2877/06/$17.00

these ways, mitochondria regulate living and death in a variety of manners [1].

Aging is the most common risk factor of the development of age-dependent neurodegenerative disorders including Alzheimer's disease (AD). However, there is no clear answer to the question of how aging becomes a risk factor of AD. Components that constitute cells including proteins, nucleic acids, and lipids are believed to degenerate with aging and their degeneration causes the degeneration of tissues and the senescence of individuals. Oxidative stress has been shown to be the primary cause for such degeneration. In eukaryotes, 90% of oxygen is used for energy metabolism primarily in mitochondria. In this process, ROS is generated as a by-product in energy metabolism. Therefore, the cell should be protected by some mechanisms to reduce this oxidative stress inside and outside mitochondria. If these protective mechanisms are exhausted, aging may be accelerated, thus increasing the risk of neurodegenerative disorders including AD.

In this review, we would like to discuss a specific decrease in activity of cytochrome *c* oxidase (COX), which is the terminal oxidase in the respiratory chain and interaction of COX with amyloid β peptide (Aβ) in AD. Moreover, we would like to emphasize the role of mitochondrial aldehyde dehydrogenase 2 (ALDH2), which has been believed to be involved in only alcohol metabolism, in the pathogenesis of AD.

2. Decrease in cytochrome *c* oxidase activity in AD patients

It has been well-known that glucose consumption is low in the brain of patients with AD, leading to a decline of energy production [2]. However, many investigators seem to have understood the decrease in energy metabolism as a secondary effect of neuronal changes toward death rather than a cause of AD. With regard to mitochondrial dysfunction, a specific decrease in COX activity has been suggested [3]. COX is an enzyme that functions in the terminal step of the electron transfer system and reduces oxygen molecules into water. It is a large complex composed of 10 subunits of nuclear gene-products and 3 subunits of mitochondrial gene-products. As compared with controls, mean protein concentration of four subunits, including mitochondrial gene- and nuclear gene-products, were significantly decreased in the brain of AD patients [4]. Since COX activity is reduced even in platelet mitochondria as well as brain mitochondria in AD patients, a decrease in COX activity cannot simply be explained as the secondary effect [5–7]. Additionally, symptoms resembling those of AD can be presented by a treatment with a COX inhibitor, azide [8].

2.1. Defect on the assembly of cytochrome c oxidase

We have long directed attention to dihydrolipoamide succinyltransferase (DLST), a component of α-ketoglutarate dehydrogenase complex in the mitochondrial Krebs cycle. Since the *DLST* gene is located in the region where a candidate gene for a familial AD is located [9], we paid attention to the *DLST* gene as a candidate gene responsible for the familial AD. As a result, the responsible gene of the familial AD was not DLST but was presenilin-1. However, since a frequency of a *DLST* haplotype in sporadic AD was significantly higher than that of controls, it is suggests that the haplotype is a risk factor for sporadic AD [10]. This correlation between the *DLST* haplotype and AD was also reported from the other groups [11,12], but negative results have also been presented [13]. This discrepancy may be due to a weak risk for AD.

By further analyzing the *DLST* gene, we clarified that the *DLST* gene encodes two gene products, one of which, named MIRTD (a mitochondrial respiratory complex assembler of truncated DLST), mediates the molecular assembly of the respiratory complexes including COX [14]. MIRTD mRNA is transcribed from intron 7 (Fig. 1A). While DLST (exons 1–15) is located in the mitochondrial matrix, MIRTD (exons 8–15) is located in the intermembrane space of mitochondria (Fig. 1B). mRNA of MIRTD was significantly decreased in the brain of AD patients compared with age-matched controls (Fig. 2A).

When MIRTD was knocked-down to evaluate the function of MIRTD, the steady state level of subunits of COX markedly decreased, accompanying a modest decrease in the respiratory complex I, leading to the decline of oxygen consumption. Since translation of these subunits was normal, the decrease of the MIRTD protein results in the defect of their assembly (Fig. 2B). Thus, full-length DLST and MIRTD, which are both gene products derived from the *DLST* gene, are both involved in mitochondrial energy metabolism, one (full length DLST; exons 1–15) as a rate-regulating enzyme of the Krebs cycle in the matrix, and the other (MIRTD; exons 8–15) by mediating predominantly the molecular assembly of COX in the intermembrane space [14]. Since the knocked-down of MIRTD predominantly decreased in all the subunits of COX including nuclear

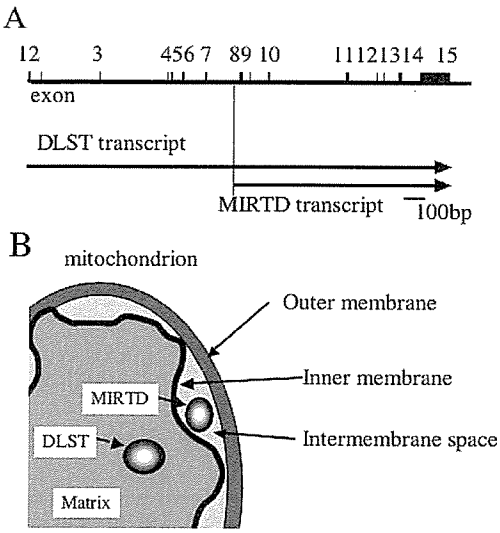

Fig. 1. The *DLST* gene bifucntionally encodes two gene-products. (A) Structure of the *DLST* gene composed by 15 exons. The novel gene product, named MIRTD, is transcribed from intron 7. (B) The Proteins are synthesized by the same reading frame. Full length DLST is present in the mitochondrial matrix, while MIRTD (exons 8–15) with about half the length on the C-terminal side, is present in the intermembrane space.

gene- and mitochondrial gene- products, this finding agrees with the results in ref [4].

To summarize the above observations, *DLST* gene polymorphisms, observed more frequently in patients with AD, reduce the expression of MIRTD, mediate the molecular assembly of COX, and decline activity of the mitochondrial respiratory chain. In addition, as oxidative stress reduced the expression of MIRTD mRNA, the quantity of MIRTD is more likely to be regulated not only by the *DLST* polymorphisms but also by many internal and external environmental factors. In some patients, MIRTD was markedly reduced in their brain regardless of the *DLST* polymorphism. Particularly, no expression of MIRTD was observed in the brain of half the patients with AD. The decrease in COX activity in the brain of AD patients can be, at least in part, explained by the decrease in MIRTD [14].

2.2. *Inhibition of COX activity by Aβ*

The COX activity is a rate-limiting step of mitochondrial energy metabolism, and its decline reduces the ATP synthesis in the cell. Therefore, the decrease in COX activity is sufficient to induce cell death. However, it does not explain how the decrease in COX involves AD. COX is located in the mitochondrial inner membrane. Aβ has recently revealed to exist inside mitochondria and several groups have recently reported that Aβ inhibits COX activity [15–17]. In addition, γ-secretase, which digests Aβ out from amyloid precursor protein (APP), was also reported to exist inside mitochondria, indicating the possibility that at least a part of Aβ are generated in mitochondria [18]. This inhibition of COX activity by Aβ may induce the generation of ROS by not only reducing energy metabolism but also arresting the electron transfer system.

3. Aβ-binding alcohol dehydrogenase and Aβ

Recently, an alcohol dehydrogenase in mitochondria was revealed to play an important role in AD. Aβ-binding alcohol dehydrogenase (ABAD) was shown to directly link Aβ to mitochondrial dysfunction [19]. On crystal structure analysis of the ABAD-Aβ complex performed in the presence of NAD^+, the three-dimensional structure of the binding site in ABAD was markedly changed when it was bound to Aβ, and its binding activity with NAD^+ was abolished. In contrast, a peptide that is derived from ABAD specifically inhibited the ABAD-Aβ interaction and then suppressed Aβ-induced apoptosis and ROS generation. A mutant APP gene and the ABAD gene were introduced into transgenic mice to enhance the Aβ production. In the transgenic mice, an increase in oxidative stress in neurons was accompanied with memory loss [19]. These results indicate that Aβ affected mitochondrial function by binding to ABAD. Thus, the ABAD-Aβ interaction can be a therapeutic target of AD.

In addition, a decrease in ATP production was accompanied with increases in ROS generation and apoptosis in transgenic mice that overexpressed a mutant form of APP [20]. The increase in ROS correlated with a decrease in COX activity. When COX activity is inhibited, more ROS should be generated. Thus, the decrease in COX activity by ABAD bound to Aβ may promote the generation of ROS. ROS enhances the toxicity of Aβ [21]. Thus, the recent reports agree with the previous findings and linked mitochondrial function to Aβ in AD.

Correlations among the contributors are summarized in Fig. 3.

4. Contribution of a decrease in ALDH2 activity to onset of AD

Mitochondria are a major source of ROS generation as mentioned above. Superoxide radicals are converted

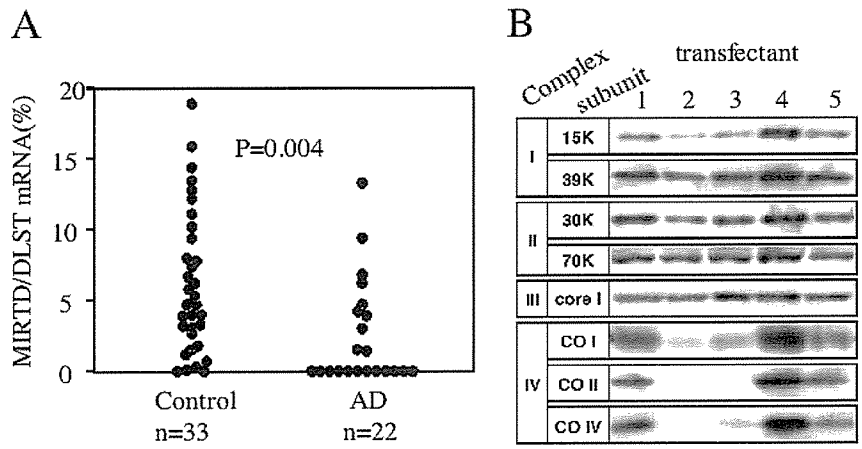

Fig. 2. Decrease in MIRTD expression in the brains of AD patients and decrease in MIRTD results in defect in the molecular assembly of the respiratory complexes. (A): Expression of MIRTD in the brains of AD patients and elderly individuals obtained by autopsy. The ratio between amounts of MIRTD mRNA and those of DLST mRNA was evaluated. The amounts of MIRTD mRNA shows a wide individual variation, but it was significantly lower in the brains of AD patients than those in the controls, and MIRTD mRNA could not be detected in the brains of half the patients (B): Defect in the molecular assembly of complexes I and IV (cytochrome *c* oxidase) in cultured cells by the knocked-down expression of MIRTD. Clones 2 and 3 are cell lines that express less MIRTD. The others are control cell lines. The decrease in the subunits was apparent in complex IV (COX). COI and COII are mitochondrial gene products, and COXIV is a nuclear gene product. All were synthesized normally, suggesting a defect in molecular assembly.

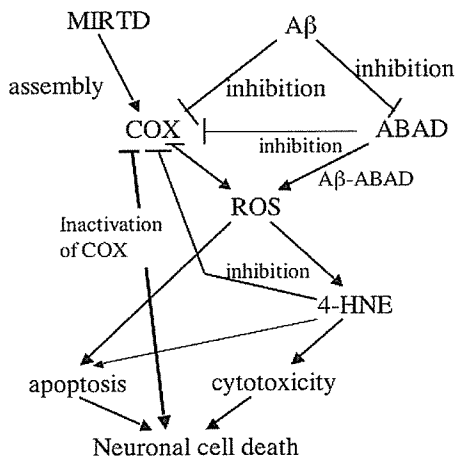

Fig. 3. Interrelations among MIRTD, COX, Aβ, and ABAD in mitochondria. Since MIRTD regulates the molecular assembly of COX, COX activity would be reduced by a decrease in MIRTD. Aβ inhibits COX activity and enhances ROS generation. Aβ also reduces the activity of ABAD and enhances the ROS generation. ROS produces toxic 4-HNE via lipid peroxides.

rapidly to hydrogen peroxides by Mn-superoxide dismutase (Mn-SOD) then to water by catalase or glutathione peroxidase. Superoxide-produced in mitochondria does not have so strong oxidative activity and does not directly damage DNA or proteins. However, as knocking-out of Mn-SOD exerts serious effects primarily on the nervous system, superoxide is undoubtedly very toxic to neurons [22]. However, how these ROS cause cell death is poorly understood. Our study on ALDH2 provided clues to the clarification of the relationship between ROS and AD [23].

4.1. *The dominant-negative ALDH2 by a genetic polymorphism*

Aldehyde dehydrogenases belong to a large family consisting of at least 16 different genes in humans, and are involved in metabolic systems of various alcohols and aldehydes according to their expression distribution and substrate specificity [24]. Among them, the *ALDH2* gene is located on chromosome 12q24.2 and codes for an enzyme consisting of a tetramer localized in the mitochondrial matrix. ALDH2 has two genetic variants, i.e., active ALDH2*1 and inactive ALDH2*2, and their structural difference is the replacement of glutamate at the 487th position by lysine by a single nucleotide substitution [25]. When even one component of the tetramer of ALDH2*1 is replaced by ALDH2*2, its binding ability with NAD^+, a coenzyme, is reduced due to a structural change, resulting in loss of the enzyme activity [26]. Therefore, ALDH2*2 acts in a dominant-negative manner, and if ALDH2*1 and ALDH2*2 are present at an equal ratio, the enzyme activity should be reduced to 1/16 (Fig. 4). This ALDH2

Table 1
Frequencies of ALDH2 genotypes in AD patients and controls

Subjects	Number of genotype [frequency]			
	1/1	1/2	2/2	1/2 & 2/2
Patients ($n = 447$)	232 [0.519]	183 [0.409]	32 [0.072]	215 [0.481]*
Controls ($n = 447$)	280 [0.626]	138 [0.309]	29 [0.065]	167 [0.374]

The frequencies of the *ALDH2*1* and *ALDH2*2* alleles were 0.724 and 0.276 in the AD patients but were 0.781 and 0.219 in the controls ($p = 0.005$). *$p = 0.001$, OR = 1.6 (95% C.I. = 1.19–2.03).

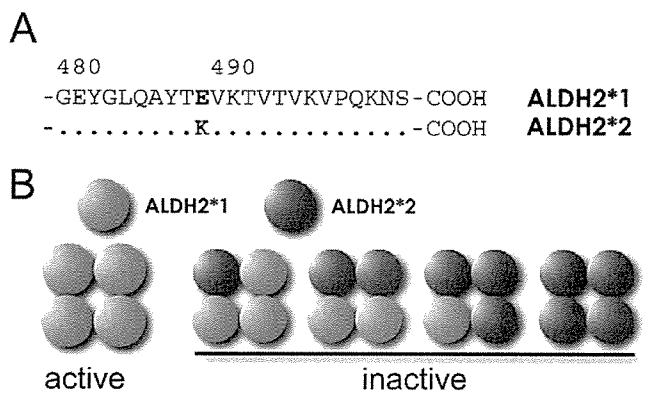

Fig. 4. *ALDH2* gene polymorphism. A: C-terminal amino acid sequence of ALDH2. Single base substitution of the *ALDH2* gene makes the enzyme active (ALDH2*1) or inactive (ALDH2*2). B: ALDH2 forms a tetramer consisting of the same subunit. Since the enzyme activity is lost if even one of the subunits is the inactive variant, ALDH2*2 acts in a dominant-negative manner.

catalyzes a low concentration of acetaldehyde as a substrate. When drinking ethanol, ALDH2 oxidizes acetaldehyde, generated by the oxidation of ethanol by alcohol dehydrogenase (ADH), into acetate. For this reason, if the ALDH2 activity is low, acetaldehyde accumulates in drinking and causes symptoms characteristic in those susceptible to the effects of alcohol such as facial flushing, nausea, and tachycardia. The presence of the inactive ALDH2*2 allele is limited to East Asian races, the Mongoloids. In the Japanese, about 30% have heterozygous ALDH2*2 allele with low ALDH2 activity, and about 10% are ALDH2*2 homozygotes having no ALDH2 activity [27].

4.2. *ALDH2*2 allele is a risk factor for late-onset Alzheimer's disease*

We analyzed *ALDH2* gene polymorphisms in 472 AD patients whose onset was later than 65 years and 472 non-demented controls [28]. The frequencies of *ALDH2* gene polymorphisms vary widely among countries and even among regions in Japan. Additionally, the frequencies of gene polymorphisms related to gerontological disorders are expected to change with aging. In fact, the genotype frequency varied depending upon age [37]. Therefore, the controls were matched not only for gender and age but also for the region. Table 1 shows the results. The percentage of individuals having at least one *ALDH2*2* allele was 48.1% in the AD group but was 37.4% in the non-demented control group. The odds ratio was 1.6, and the p value was 0.001, indicating sufficient significance. The results were similar also when analysis was performed separately for males and females, and no gender difference was noted.

An allele of Apolipoprotein E (ApoE), ApoE-ε4 is widely accepted to be a risk factor for late-onset AD and the odds ratio of the onset of AD in individuals having the *APOE-ε4* allele is about 3.0. Figure 4 shows the results of cross comparison of APOE gene polymorphisms and ALDH2 gene polymorphisms. These results indicate that the coexistence of the *APOE-ε4* allele and *ALDH2*2* allele synergistically increases the frequency of the onset of AD (Fig. 5). Particularly, the frequency of the onset of AD was 31 times higher in individuals being *APOE-ε4* homozygous and having at least one *ALDH2*2* allele than in those having neither allele. About 0.6–1% of Japanese are estimated to belong to the group with the combination of these genotypes, and nearly all of them are expected to develop

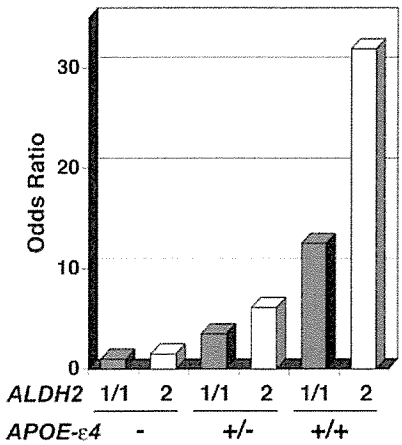

Fig. 5. Synergism between *ALDH2*2* and *APOE-ε4* in the risk for the occurrence of sporadic AD. Concerning ALDH2, (1/1) means homozygotes of the *ALDH2*1* allele, and (2) means homozygotes or heterozygotes having the *ALDH2*2* allele. Concerning APOE-ε4, (−) means individuals having no *ε4* allele, (+/−) means heterozygotes of the *ε4* allele, and (+/+) means homozygotes of the *ε4* allele. The odds ratio of the occurrence of AD is 31 times higher in individuals having the *ALDH2*2* allele and being homozygous concerning the *ε4* allele than in those having neither allele.

AD on the basis of calculation. The age at onset was also significantly accelerated by the synergy between *APOE-ε4* and *ALDH2∗2* [28].

The reproducibility of the findings that the *ALDH2∗2* allele is a risk factor for AD and that the risk is synergistically enhanced by its coexistence with *APOE-ε4* has been confirmed by the results of Tamaoka et al. of Tsukuba University using samples from patients after pathological definitive diagnoses (Tamaoka et al., 2003; Annual meeting in Japanese Society of Dementia Research). While *ALDH2* gene polymorphisms were also analyzed in Korea as a possible risk factor for AD, the cognitive ability was reported to have been unrelated to the ALDH activity [29]. However, the lack of statistical significance in this report, analyzing only 60 AD patients, is not persuasive because of an insufficient size.

4.3. ALDH2∗2 allele and increase in oxidative stress

Since the sensitivity to alcohol markedly depends upon *ALDH2* gene polymorphisms, the incidences of disorders due to excessive alcohol intake such as alcoholism and alcoholic hepatitis are low in individuals having the *ALDH2∗2* allele [30]. It has also been reported that the *ALDH2∗2* allele is a risk factor for polyneuropathy in diabetes mellitus, tumor, hypertension, and myocardial infarction [31–34]. However, since the gene polymorphisms of ALDH2 are closely related to the lifestyle factor of drinking, it is difficult to distinguish the direct effect caused by gene polymorphisms from the secondary effects by ethanol consumption. This distinction is very important, because it is related to whether drinking should be recommended from the prophylactic viewpoint. We, therefore, strictly evaluated changes in individuals with the *ALDH2∗2* allele by eliminating the effect of alcohol intake. In the large-scale epidemiological study by the Department of Epidemiology, National Institute of Longevity Science [35,36], a medical check consisting of blood tests, urinalysis, and investigation of the lifestyle including ethanol consumption and clinical history was performed in about 2,300 healthy individuals aged in their 40s to 70s randomly selected from local residents. We performed a genetic analysis on the *ALDH2* polymorphisms and searched phenotypes specific in individuals with *ALDH2*2* allele in this cohort. Many phenotypes specific to the carriage of *ALDH2*2* were found in such serum levels of lipoproteins, but these phenotypes were correlated with ethanol intake, thus due to the drinking habit, but not to the direct genetic effect. As a result, the serum level of lipid peroxides (LPO) was significantly increased in females having the *ALDH2∗2* allele even after normalizing with ethanol consumption to exclude the effect of alcohol intake. This result suggests the possibility that reduced ALDH2 activity increases oxidative stress independently of alcohol intake and that the *ALDH2∗2* allele may be a risk factor for many age-associated diseases [37]. No significant difference was observed in males, but it was probably because the effect of alcohol intake on the accumulation of LPO was excessive. The next question is what effect *ALDH2* gene polymorphisms have in AD.

4.4. Molecular mechanism of the promotion of the onset of AD by ALDH2∗2

As observed above, epidemiological investigations have demonstrated that the presence of the *ALDH2∗2* allele increases oxidative stress and is a risk factor for AD. Since the increase in oxidative stress is independent of alcohol metabolism, ALDH2 is considered to suppress oxidative stress by metabolizing substrates other than acetaldehyde. Additionally, as ALDH2 is localized in mitochondria, it is considered to metabolize aldehydes generated in mitochondria. Then, the next question is what is the aldehyde derivative.

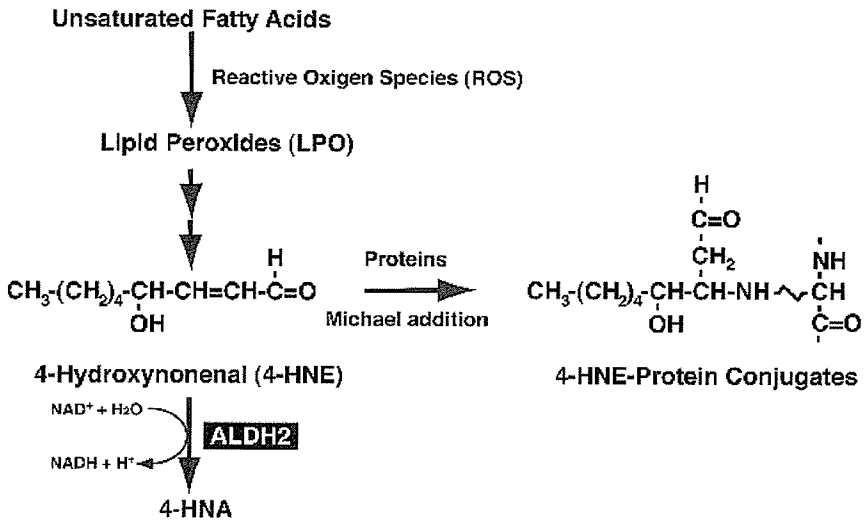

Fig. 6. Mechanism of the formation of trans-4-hydroxy-2-nonenal (4-HNE) and its oxidation by ALDH2. 4-HNE is spontaneously generated from lipid peroxides and is oxidized by ALDH2. 4-HNE is highly cytotoxic, because it modifies proteins and nucleic acids and inactivates them.

LPO is generated by peroxidation of unsaturated fatty acids with ROS. From these LPO, aldehydes such as marondialdehyde (MDA), which is a marker of oxidative stress, and highly toxic 4-hydroxy-2-nonenal (4-HNE) are spontaneously generated, where MAD and 4-HNE are aldehyde derivatives. Particularly, 4-HNE causes protein denaturation by readily binding with lysine, histidine, serine, and cysteine residues [38]. In fact, 4-HNE reduces Na^+,K^+-ATPase activity [39]. It has also been shown *in vitro* to promote neuronal death [40]. Moreover, the accumulation of LPO and 4-HNE has been reported in neurodegenerative disorders including AD and Parkinson's disease [41–43].

Thus, we hypothesized that ALDH2 is involved in the detoxification of 4-HNE generated by oxidative stress of mitochondria and that defects in the ALDH2 activity cause neuronal death by stimulating the accumulation of 4-HNE due to oxidative stress. The hypothesis is summarized as follows: (a) ALDH2 detoxifies 4-HNE by oxidizing its aldehyde group; (b) in individuals with reduced ALDH2 activity, 4-HNE accumulates because of insufficient detoxification; (c) mitochondrial respiratory chain enzyme activities are inhibited by the accumulation of 4-HNE, and then the frequency of the generation of ROS increases; (d) ROS produces LPO and 4-HNE is generate by spontaneous reaction (Fig. 6).

To verify this hypothesis, we prepared a mouse/rat-version *ALDH2*2* gene and introduced it into rat PC12 cells. As a result in a dominant negative manner, ALDH2 activity was suppressed in the cells into which the *ALDH2*2* gene was introduced, and cell death was induced readily by 4-HNE [44] (Fig. 7B). The death of cells with defective in ALDH2 activity was promoted when ROS production was forcibly induced with antimycin A, which is an inhibitor of complex III of the mitochondrial respiratory chain. In this experiment, marked accumulation of 4-HNE was observed in the cells with reduced ALDH2 activity [44] (Fig. 7A). It is possible to interpret that other enzymes could increase to compensate for the loss of ALDH2. However, since 4-HNE is an aldehyde derivative, it is reasonable that ALDH2 oxidizes 4-HNE. These results support the above hypothesis and indicate the role of ALDH2 protective against the mitochondrial oxidative stress [44].

ALDH2 has been discussed conventionally in relation only to ethanol drinking or its metabolism. However, as animals that do not drink also have the same gene, ALDH2 should be considered to have an intrinsic function other than ethanol-acetaldehyde metabolism. On the basis of the results we have obtained, it appears reasonable to think that ALDH2 is one of the protective mechanisms against oxidative stress [23].

4.5. *Age-dependent degeneration of the central nervous system in ALDH2-suppressed transgenic mice*

Construction of model animals by genetic manipulations is one of the best methods for analysis of the

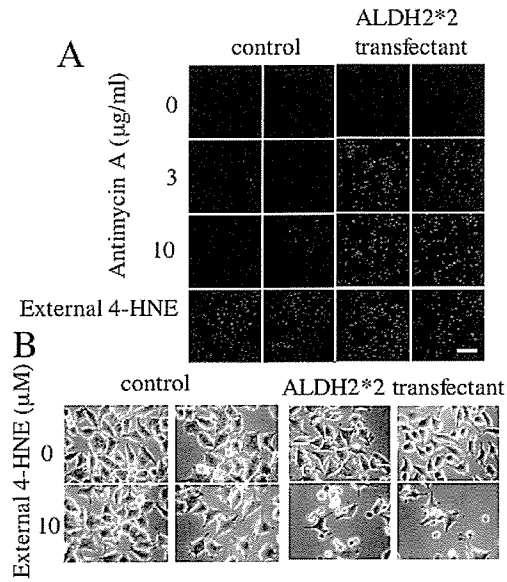

Fig. 7. Transfection of inactive *ALDH2*2* into PC12 accumulates 4-HNE after forced generation of ROS and made cells sensitive to 4-HNE (see ref. [44] for details). (A) Accumulation of 4-HNE after treatment with antimycin A was imaged by confocal scanning laser microscopy. PC12 cells were stably transfected with the *ALDH2*2* gene or an empty vector. Transfectants were treated with the indicated concentration of antimycin A to induce ROS or 1 μM of external 4-HNE, and incubated for 24 h. After fixation, cells were stained with anti-4-HNE antibody. Scale bar; 200 μm. Marked accumulation of 4-HNE was observed in transfectants in which ALDH2 activity was suppressed. (B): 4-HNE caused marked cell death in PC 12 stable transfectants in which ALDH2 activity was suppressed in a dominant-negative manner by introducing the *ALDH2*2* gene at concentrations that caused no death in the parent and control transfectants retaining ALDH2 activity. PC12 or each transfectant was treated with 10 μM 4-HNE or ethanol (1/1000 volume of medium) as a control (0 μM). One day after treatment, cells were observed under a phase-contrast microscope (x 200). Scale bar; 50 μm.

involvement of particular genes in the defense against oxidative stress at the animal level. In fact, in mice defective in Mn-SOD, oxidative stress accumulates, and mitochondrial dysfunction and subsequent cell death are observed [22]. Since the model mice die about 1 week after birth, and analysis of age-dependent changes is impossible, this type is too sever to investigate age-dependent degeneration. Recently, prolongation of life was reported in mice into which the catalase gene equipped with a target sequence of mitochondria was introduced [45]. This finding clearly indicates the importance of the control of oxidative stress in aging.

We constructed ALDH2-deficient mice by introducing a mutant *ALDH2*2* gene. As mentioned above, ALDH2 belongs to a large family of aldehyde dehydrogenases. For aldehydes including 4-HNE, which are detoxified by ALDH2, there are multiple detoxification systems such as glutathione in addition to ALDH2. Knocking-out one such gene is likely to cause little change in aldehyde metabolism, because the knocked-out enzyme would be complemented with other members of the gene family. In fact, in ALDH2 knock-out mice, methoxyacetaldehyde (MALD) metabolism is reduced markedly, but no abnormality is observed in the development process or physical functions [46]. In humans, on the other hand, the suppression of ALDH2 activity by ALDH2*2 causes various disorders presumably due to increased oxidative stress. For example, the risk of the occurrence of AD is higher in individuals with the *ALDH2*2* allele. Therefore, we expected the development of model animals closer to humans by introducing the *ALDH2*2* gene and dominant-negatively suppressing the ALDH2 activity.

We first prepared transgenic mice by introducing the mouse-version of the *ALDH2*2* gene under a strong promoter which enhances ubiquitous expression. We named the resultant mice DAL (Dominant negative of ALDH2) mice. These mice showed no abnormality in the developmental process even when maintained as homozygotes. Females exhibited no particular abnormality on physical examinations compared with C57BL/6 mice when observed until 24 months after birth. A DAL line exhibited specific expression of the ALDH2*2 gene in hipocampus and cortex, nevertheless we used a promoter which enhances ubiquitous expression. Therefore, whether central neurons were vulnerable to 4-HNE similarly to PC12 cells was also evaluated. The cerebral cortex was removed from DAL mice at embryonic day 16, and 4-HNE was added to its primary culture. Neuronal death was promoted in DAL mice, suggesting an increase in oxidative stress in the brain (manuscript in preparation).

Females, which showed no apparently different phenotype compared with C57BL/6 mice, were particularly analyzed. Autopsy of the brain was performed in 6-month-old mice, but no difference compared with the brain of C57BL/6 mice was noted. However, in 18-month-old DAL mice, signs of neurodegeneration such as atrophy of the hippocampus and associated loss of pyramidal neurons and activation of glial cells were observed (Fig. 8). These changes began to be observed sporadically at the age of 12 months and increased with aging. However, no marked difference was observed in motor functions or sensory functions between DAL mice and control C57BL/6 mice. Therefore, the mice were tested using the water maze task, which is widely used as a test of spatial cognitive ability, which is re-

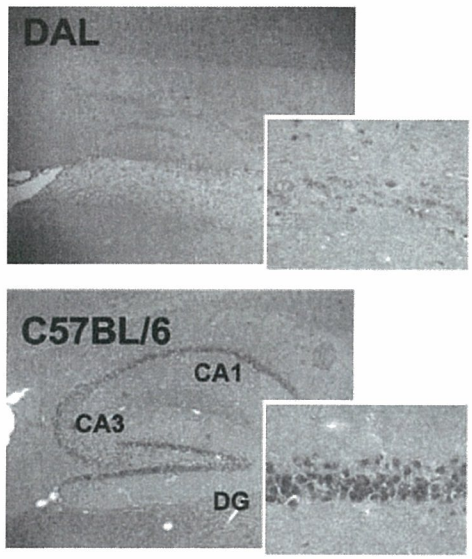

Fig. 8. Hippocampal atrophy and pyramidal cell degeneration in DAL mice. In DAL mice (females), marked hippocampal atrophy and pyramidal cell degeneration were observed at the age of 18 months by H & E stain. Inserts are expansions of the CA1 region.

lated to the hippocampus. DAL mice exhibited a decrease in spatial cognitive ability at the age of 6 months and a marked decrease at the age of 18 months. Such brain degeneration and decrease in spatial cognitive ability are considered to be due to reduced resistance to oxidative stress similar to the neurons in the primary culture. We are analyzing age-dependent changes in oxidative stress markers such as 4-HNE. Actually, in DAL mice expressing ALDH2∗2 in a muscle-specific manner, signs of muscle atrophy and associated mitochondrial abnormalities and accumulation of 4-HNE were noted (manuscript in preparation).

4.6. *4-HNE metabolized by ALDH2 and its contribution to AD*

From the above observations, we propose that the *ALDH2∗2* allele is a risk of AD, because highly toxic aldehydes such as 4-HNE accumulate in the brain due to age-dependent increases in oxidative stress, and suppression of ALDH2 activity promotes the onset of AD (Fig. 9). This leads us to two questions. First, do aldehydes such as 4-HNE accumulate before the onset of AD? Recently, marked increases in 4-HNE were reported in the hippocampus and superior and middle temporal gyrus of patients with mild cognitive impairment (MCI) and those with early AD compared with healthy individuals [47]. These results, which are in agreement with the results of analysis of LPO in cerebrospinal fluid [48], suggest that accumulation of oxidative stress, typically represented by 4-HNE, occurs before the onset of AD. Secondly, does the accumulation of aldehydes such as 4-HNE cause symptoms characteristic of AD? 4-HNE not only induces neuronal death but also causes synapse dysfunction due to mechanisms such as reducing the Na^+, K^+-ATPase activity [49] and markedly inhibits microtubule formation and neurite outgrowth [50]. Furthermore, there have been a number of reports on the relationship between neurofibrillary tangle (NFT), which is a pathological feature characteristic of AD, and oxidative stress [51]. Concerning 4-HNE, in particular, it has been reported to induce structural changes in phosphorylated tau by modifying it and to make tau a structure in NFT [52, 53], so that 4-HNE is considered to play an important role in NFT formation. Concerning senile plaques, there have been many reports on increases in oxidative stress due to Aβ but few reports on the relationship between 4-HNE and the mechanism of Aβ production. Recently, however, an increase in the quantity of BACE1 expression associated with the activation of stress response pathways by 4-HNE was reported, and the possibility that 4-HNE increases Aβ production was suggested [54]. Also, in transgenic mice, which are a model of Aβ deposition, accumulation of LPO was reported to precede accumulation of Aβ [55]. According to our epidemiological investigation, the *ALDH2∗2* allele and *APOE-ε4* allele synergistically increased the risk of AD. Concerning this association between APOE and 4-HNE, the cytoplasm of pyramidal cells was reported to be positive for 4-HNE only in individuals with the *APOE-ε4* allele on immunostaining of the brain of AD patients using anti-4-HNE antibody [56]. Moreover, the strength of binding between APOE and 4-HNE was $\varepsilon 2 > \varepsilon 3 > \varepsilon 4$, and this order was in agreement with the preventive effect of APOE against cell death due to 4-HNE [57]. From these observations, it is considered that APOE eliminates free 4-HNE in the body and that the possession of APOE-ε4, the APOE with the weakest 4-HNE elimination ability, leads to the accumulation of 4-HNE in neurons and an increase in oxidative stress. Accumulation of 4-HNE is considered to be further intensified if the ALDH2 activity is also reduced, resulting in an increase in the risk of AD.

5. Diversity of 4-HNE elimination mechanisms

Since highly toxic aldehydes such as 4-HNE are generated spontaneously by lipid peroxidation, there are a

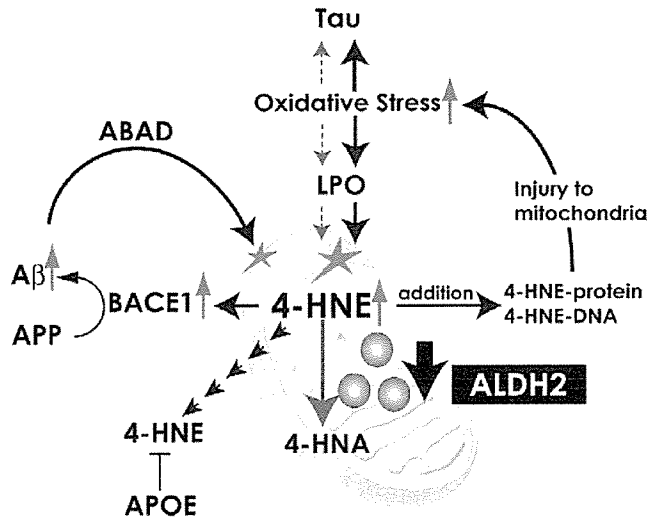

Fig. 9. A model of accumulation of 4-HNE by the suppression of ALDH2 activity and its effects. In mitochondria, a decrease in ALDH2 activity promotes the accumulation of 4-HNE caused by oxidative stress, and binding of 4-HNE with proteins and DNA induces mitochondrial disorders. Mitochondrial disorders further enhance oxidative stress. Since this process is accelerated by aging, a decrease in ALDH2 activity is a risk factor of neurodegenerative disorders including AD. Oxidative stress including 4-HNE causes phosphorylation and structural changes of tau, and promotes NFT formation. 4-HNE also increases the expression of BACE1 and promotes the accumulation of Aβ. Furthermore, Aβ binds with ABAD and damages mitochondria. On the other hand, APOE promotes the elimination of 4-HNE.

variety of mechanisms for their elimination including oxidation by ALDH2, etc., reduction by aldose reductase, etc. [58], and binding with glutathione [59]. We recently discovered that ADH polymorphism is a risk factor for cerebral infarction [60]. The possible involvement of ADH in the reduction of 4-HNE has been suggested by a study using hepatocytes [61], and this study must be extended to the nervous system. Also, multiple aldehyde dehydrogenases are considered to oxidize 4-HNE, and the report that ALDH5A present in mitochondria, as is ALDH2, plays an important role in the detoxification of 4-HNE in the central nervous system is interesting [62].

DAL mice gradually develop neurodegeneration with aging after the growth period. Analysis of these mice may clarify the relationship between lesions characteristic of AD and oxidative stress. Also, the development of appropriate methods for the prevention of lesions occurring in these mice is considered to provide clues to the development of prophylactic and therapeutic methods against diseases including AD. Figure 9 summarizes our conclusion.

6. Concluding remarks

Reports of the inhibition of COX activity by Aβ and generation of ROS by its binding with an ADH in mitochondria showed strong evidence that mitochondria play a direct role in the pathogenesis of AD. Also, our results that amounts of MIRTD, which mediates the molecular assembly of the respiratory complexes including COX, was low in the brain of AD patients were in agreement with these previous reports. The findings that ALDH2 is a risk factor for AD and that it acts as a protective mechanism against oxidative stress contributed to the clarification of the role of mitochondria from a novel view. Since transgenic mice with the declined ALDH2 activity showed age-dependent neurodegeneration accompanying memory-loss, analysis of these mice is expected to clarify the relationship between lesions characteristic of AD and oxidative stress.

References

[1] S. Ohta, A multi-functional organelle mitochondrion is involved in cell death, proliferation and disease, *Curr. Med. Chem.* **10** (2003), 2485–2494.
[2] R.H. Swerdlow and S.J. Kish, Mitochondria in Alzheimer's disease, *Int. Rev. Neurobiol.* **53** (2002), 341–385.
[3] I. Maurer, S. Zierz and H. Moller, A selective defect of cytochrome c oxidase is present in brain of Alzheimer disease patients. *Neurobiol. Aging* **21** (2000), 455–462.
[4] S.J. Kish, F. Mastrogiacomo, M. Guttman, Y. Fukukawa, J-W. taanman, S. Dozic, M. Pandolfo, J. Lamarche, L. DiStefano and L.-J. Chang, decreased Brain Protein Levels of